

Potential profile near singularity point in kinetic Tonks-Langmuir discharges as a function of the ion sources temperature

L. Kos,¹ D. D. Tskhakaya, Sr.,^{2,a)} and N. Jelić²

¹LECAD Laboratory, Faculty of Mechanical Engineering, University of Ljubljana, SI-1000 Ljubljana, Slovenia

²Association EURATOM-ÖAW, Institute for Theoretical Physics, University of Innsbruck, A-6020 Innsbruck, Austria

(Received 16 February 2011; accepted 12 April 2011; published online 31 May 2011; publisher error corrected 6 June 2011)

A plasma–sheath transition analysis requires a reliable mathematical expression for the plasma potential profile $\Phi(x)$ near the sheath edge x_s in the limit $\varepsilon \equiv \lambda_D/\ell = 0$ (where λ_D is the Debye length and ℓ is a proper characteristic length of the discharge). Such expressions have been explicitly calculated for the fluid model and the singular (cold ion source) kinetic model, where exact analytic solutions for plasma equation ($\varepsilon = 0$) are known, but not for the regular (warm ion source) kinetic model, where no analytic solution of the plasma equation has ever been obtained. For the latter case, Riemann [J. Phys. D: Appl. Phys. **24**, 493 (1991)] only predicted a general formula assuming *relatively high* ion-source temperatures, i.e., much higher than the plasma-sheath potential drop. Riemann’s formula, however, according to him, never was confirmed in explicit solutions of particular models (e.g., that of Bissell and Johnson [Phys. Fluids **30**, 779 (1987)] and Scheuer and Emmert [Phys. Fluids **31**, 3645 (1988)]) since “the accuracy of the classical solutions is not sufficient to analyze the sheath vicinity” [Riemann, in *Proceedings of the 62nd Annual Gaseous Electronic Conference, APS Meeting Abstracts*, Vol. 54 (APS, 2009)]. Therefore, for many years, there has been a need for explicit calculation that might confirm the Riemann’s general formula regarding the potential profile at the sheath edge in the cases of regular *very warm* ion sources. Fortunately, now we are able to achieve a very high accuracy of results [see, e.g., Kos *et al.*, Phys. Plasmas **16**, 093503 (2009)]. We perform this task by using both the analytic and the numerical method with explicit Maxwellian and “water-bag” ion source velocity distributions. We find the potential profile near the plasma–sheath edge in the *whole range* of ion source temperatures of general interest to plasma physics, from zero to “practical infinity.” While within limits of “very low” and “relatively high” ion source temperatures, the potential is proportional to the space coordinate powered by rational numbers $\alpha = 1/2$ and $\alpha = 2/3$, with medium ion source temperatures. We found α between these values being a non-rational number strongly dependent on the ion source temperature. The range of the non-rational power-law turns out to be a very narrow one, at the expense of the extension of $\alpha = 2/3$ region towards unexpectedly low ion source temperatures. © 2011 American Institute of Physics. [doi:10.1063/1.3587112]

I. INTRODUCTION

First, we ought to admit that during our investigations related to the present subject, we were not able to find satisfactory definitions regarding some basic terminological conventions in the field of plasma, sheath, and intermediate region problems. The most explicit answer to the question what, in the context of kinetic plasma and sheath problem for finite and vanishing ε ($\varepsilon = \lambda_D/\ell$, where $\lambda_D \equiv \sqrt{\epsilon_0 k T_e / n e^2}$ is the familiar Debye length and ℓ is a proper characteristic length of discharge), the terms of “cold” and “warm” ion sources mean, was given by Riemann only recently.⁷ He states that a “cold” source produces “new” ions by ionization or charge exchange “with negligible velocity.” In a warm source, in contrast, the energy spread of “new” ions exceeds the “width of the intermediate region.” However, this defini-

tion does not seem to be very clear because in the case of vanishing ε , the concept of “width of the intermediate region” is not applicable. So here, we adopt another “working” definition stating that a warm ion source is presented by a neutral velocity distribution function (VDF), the thermal energy spread of which is comparable to or higher than (1) its directional energy, (2) the thermal *electron* energy, and (3) the plasma potential energy drop Φ_s at the point of plasma solution singularity obtained in the limit of vanishing ε . The quantitative implications of this will become clear during the process of making necessary approximations and after examining numerical results at the end of this paper.

Solution to the plasma-sheath transition problem is a single but very important step towards finding an analytic approximate expression for the potential profile uniformly valid in the entire region of a physically bounded discharge. Achieving this goal requires an exhaustive analysis consisting of many consecutive steps, e.g., rescaling the potential profile appropriately in the so-called “intermediate scale,” in whose

^{a)}Also at Institute of Physics, Georgian Academy of Sciences, 0177 Tbilisi, Georgia.

representation the potential profiles are nearly independent on discharge parameter ϵ . Riemann has recently⁴ summarized the “state of the art” of plasma-sheath analysis showing that there are three models that should be distinguished, namely (1) fluid model, (2) kinetic model with ions generated with zero initial velocity (so-called “cold” or “singular” ion source), and (3) kinetic model with ions generated with a finite initial velocity (the so-called “warm” or “regular” ion source). While proper analysis was performed within fluid approximation and the kinetic model with “cold” ion sources, Riemann states that “the structure of the plasma-sheath transition for models with hot ion source was never analyzed!”⁴

During the last and present centuries, the plasma and sheath problem was treated via various alternative methods under various assumptions and applied approximations. On one side, the usually adopted analytic approach follows the Tonks and Langmuir T&L (Refs. 1, 8, and 9) intuitive idea (interpreted later in a mathematically correct way by Caruso and Cavaliere¹⁰) to split the problem into the so-called plasma equation and sheath equation and to solve them separately under various approximations.

Analytic matching between these solutions and exact numerical solution was found only recently by Riemann for the fluid model¹¹ as well as for both singular kinetic collision-dominated¹² and collision-free¹³ models. Computer simulations of singular kinetic models were also performed.^{14,15} Finally, the first experimental results on the plasma potential profile near the sheath edge appeared recently¹⁶ showing that in a laboratory plasma with an approximately cold, i.e., *singular* ion source, the potential is indeed proportional to the square root of the distance from the sheath edge ($\Phi - \Phi_s \propto (x - x_s)^{1/2}$), as follows from Franklin and Ockendon’s¹⁷ old considerations, elaborated further in detail by Riemann.^{11,18} However, we are here interested in a symmetric plane-parallel kinetic T&L model with *regular*, arbitrary “warm” ion source velocity distribution, where another power law and consequent scaling laws have been predicted¹ but never confirmed¹⁹ for particular explicit ion sources.

The geometry of the problem together with a schematic potential profile in the case of a negligible ϵ , together with an example of finite ϵ , is illustrated in Fig. 1. Due to the symmetry of the problem, only half of the discharge should be considered as illustrated in Fig. 2. It is necessary here to point out that the central quantity of interest in the present work is the potential profile in the so-called $\epsilon = 0$ limiting case. The final

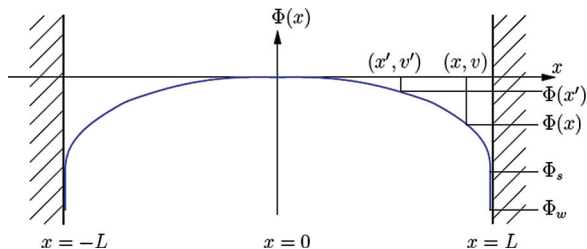


FIG. 1. (Color online) Schematic diagram of the T&L model in one-dimensional (plane) geometry with potential $\Phi(x)$. The plasma center at $x = 0$, walls at $x = \pm L$. Φ_s is the potential of the sheath edge, Φ_w is the wall potential.

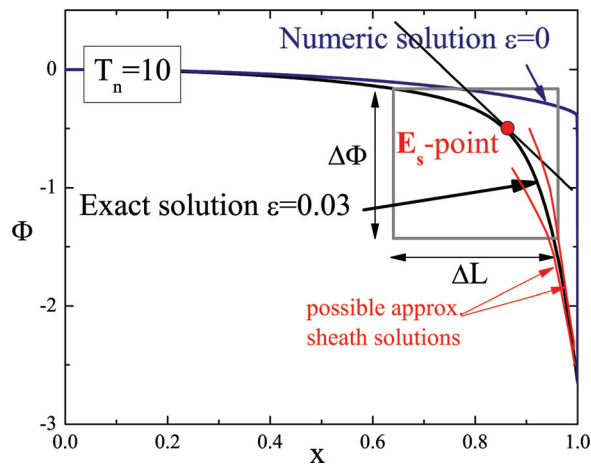


FIG. 2. (Color online) Exact solution for the plasma potential Φ (in the dimensionless form $e\Phi/kT_e \rightarrow \Phi$, with T_e the electron temperature) for $\epsilon = \lambda_D/L = 0.03$ for Maxwellian ion source temperature T_n normalized as $T_n \rightarrow T_n/T_e = 10$ in comparison with the exact numerical solution of plasma equation ($\epsilon = 0$) for the same temperature. Possible approximate sheath solutions are drawn symbolically. The squared region $\Delta L - \Delta\Phi$ is a symbolic presentation of the intermediate region or, equivalently, the uncertainty of the plasma-sheath transition around the point $E_s = \Delta\Phi/\Delta L$.

mathematical problem to be solved in the context of constructing the intermediate region appears as a kind of mathematical “perturbation” of $\epsilon = 0$ case, via small but finite ϵ . Such an explicit solution is illustrated in Fig. 2. This particular comparison of exact potential profiles with finite ϵ ’s was obtained here for the Maxwellian distributed ion source with temperature $T_n/T_e = 10$ via a highly reliable numerical computational method developed by Kos *et al.*^{6,20} for dealing with the complete T&L collisionless discharge model as well as with its special case of quasineutral plasma known as Bissell and Johnson (B&J) model.^{2,3} This method has proved as superior to others known by us in obtaining results with an extremely high resolution and at the same time being applicable to a wide (practically unlimited) range of ion source temperatures.

A logical question here arises why any approximate solution with final ϵ case should be required, if the exact solution can be obtained via a numerical calculation^{20,21} or, e.g., via particle in cell (PIC) simulations.²² However, it should be recognized that the problem *in principle* does not concern either a particular discharge with particular ϵ or a particular ion source temperature, but it should be defined and solved as a *universal* one resulting in some universal rules. In this context, the exact solution is just an auxiliary one for a comparison of how good a possible analytic approximation is, as done, e.g., in Fig. 11 in Riemann’s work with the kinetic model with the cold ion source.¹³

Furthermore, an analytic formulation of the reference point joining (or separating) plasma and sheath might be very important in plasma applications. For example, the validity of fusion-relevant codes dealing with the Scrape of Layer, like SOLPS (Ref. 23) and EDGE2D, is limited to the region bounded by a plasma-sheath surface at which fluid approach breaks. In the case of vanishing ϵ , the sheath thickness is negligible and its position coincides with the wall position with a well-defined boundary condition defined with

famous Bohm criterion,²⁴ i.e., via its generalization.²⁵ In plasmas with finite ε , the plasma sheath common boundary spreads into a region of a finite width whose placement can be estimated as a transition region around a reference point where *electric field* takes the value $E_s = \Delta\Phi/\Delta L$, where $\Delta\Phi$ and ΔL should be rather safely estimated for both theoretical analysis (see, e.g., Riemann's paper¹³ and references therein) and engineering purposes,²⁶ however for the cold ion sources. Following the exhaustive mathematical procedure by Riemann in 1991 (Ref. 1), the scaling variables $\Delta\Phi$ and ΔL yield the reference electric fields $E_s \sim \varepsilon^{-2/5}$, $E_s \sim \varepsilon^{-4/9}$, and $E_s \sim \varepsilon^{-2/7}$ (where E_s is assumed to be normalized to kT_e/eL) for fluid, cold kinetic, and warm kinetic models, respectively. A necessary prerequisite in establishment of such scaling laws is to know the exact potential profile in the so-called " $\varepsilon = 0$ model." It has been shown by Riemann¹ that the potential profile $\Phi(x)$ in front of the sheath edge in plasmas with finite ε in the kinetic model with *cold* ion source follows the law $(\Phi_s - \Phi) = C(x_s - x)^\alpha$, where subscript "s" denotes the location of the sheath edge and any corresponding quantity at that place. It will be shown in this paper that coefficient C is in fact a *function* of the ion source, so the last expression should be replaced with $(\Phi_s - \Phi) = C_{T_n}(x_s - x)^\alpha$, where C_{T_n} will be found together with α . In contrast to singular, i.e., cold ion source ($T_n = 0$) where $\alpha = 1/2$, for high enough but still unknown T_n , value $\alpha = 2/3$ is expected (e.g., Riemann¹) independently of the detailed shape of the ion-source velocity distribution, i.e., on particular value of T_n . Unfortunately, value $\alpha = 2/3$ for the warm ion-source has never been proved by, e.g., any numerical method or experimental means.

The question triggered recently by Riemann⁵ is *whether one can obtain accurate results to identify the form of the sheath edge singularity, i.e., to find safely the power α in the formula $(\Phi_s - \Phi) = C(x_s - x)^\alpha$ describing the limiting potential variation in front of the sheath edge (x_s, Φ_s)* . In order to answer this question in the present work, we employ two particular velocity distributions, namely the Maxwellian one with two different ionization mechanisms and the "water bag" shaped. The employment of the latter distribution which in adiabatic approximation fully corresponds to the fluid model (Davidson²⁷) is aimed at proving that the results really are independent of the velocity distribution shape. It turns out that, e.g., a requirement $kT_n \geq e|\Phi_s| > 0$ could be an over-restriction necessary to make analytic approximations while numerical solution shows that for T_n greater than a value of the order of one tenth of T_e . Within the narrow transition between $T_n = 0$ characterized by $\alpha = 1/2$ and $T_n > 0.05T_e \div 0.1T_e$ characterized by $\alpha = 2/3$, the plasma potential near the singularity point is characterized by a non-rational number $2/3 > \alpha > 1/2$. In many plasmas of interest, the temperature T_n might fall exactly within this region and this might be a source of problem, e.g., in applying any universal rule to a plasma whose neutral temperature is even one order of magnitude or greater than the room temperature.

Section II presents theoretical investigations on the potential profile near the point of singularity for the cases of Maxwellian and water-bag distributions. Section III describes the numerical method. Section IV presents main

results of numerical solutions. Section V brings a summary with conclusion.

II. THEORETICAL CONSIDERATIONS

We deal with a plane-parallel discharge of the T&L type⁸ as sketched in Fig. 1. The properties of T&L discharge have been analytically investigated as performed in works by Franklin and Ockendon¹⁷ and Riemann¹ via employing mathematical tools elaborated in books by van Dyke²⁸ and Kaplan.²⁹ These properties were found for a general ion velocity distribution while we concentrate here on Maxwellian and "water-bag" distributions as good candidates to take the role in a variety of discharges. For the ion density in such a discharge, one obtains the general expression (see the details in, e.g., Ref. 20)

$$\frac{n_i(x)}{n_0} \rightarrow n_i(x) = 2B \int_0^\infty dv \int_0^1 \frac{dx'}{\sqrt{v'^2}} \times F_n \left(-\frac{\sqrt{v'^2}}{v_{T_n}} \right) \exp \left\{ \frac{\beta e \Phi(x')}{kT_e} \right\} H(v'^2), \quad (1)$$

where

$$B = \frac{1}{2\pi} \sqrt{\frac{1}{T_n} \frac{m_i}{m_e} \frac{n_0}{n_{e,av}}} \exp \left\{ \frac{e\Phi_w}{kT_e} \right\} = \frac{1}{\sqrt{T_n}} B_0, \quad (2)$$

$$\tau = \frac{T_e}{T_n} = \frac{1}{T_n}, \quad v_{T_{ni}} = \sqrt{\frac{kT_{n,i}}{m_i}}, \quad \frac{x}{L_i} \rightarrow x,$$

$$v'^2 = v^2 - \frac{2e}{m_i} \{ \Phi(x') - \Phi(x) \},$$

where subscripts "n," "i," and "e" denote neutrals, ions, and electrons, respectively, $L_i = c_s/v_i$ (v_i is the ionization frequency, $c_s = \sqrt{kT_e/m_i}$), $H(z)$ is the Heaviside step-function, and $\beta = 0, 1, 2, \dots$, denotes uniform, proportional to electron density and proportional to square of electron density ionization profiles, respectively. The symmetric auxiliary distribution function $F_n(v)$ of neutrals is connected with their velocity distribution function $f_n(v)$ with the relation

$$F_n \left(\frac{v}{v_{T_n}} \right) = \sqrt{2\pi} v_{T_n} f_n \left(\frac{v}{v_{T_n}} \right), \quad (3)$$

$$F_n(-z) = F_n(z).$$

Further, we use the following non-dimensional variables:

$$\frac{v}{\sqrt{2}c_s} \rightarrow v, \quad \frac{e\Phi(x)}{kT_e} \rightarrow \Phi(x), \quad \frac{n_i}{n_0} \rightarrow n. \quad (4)$$

For the **Maxwellian ion source**, the auxiliary function (3) is

$$F_n \left(\frac{v}{v_{T_n}} \right) = \exp \left\{ -\frac{v^2}{2T_n} \right\} \quad (5)$$

and the ion density equals

$$n_i(x) = B \int_0^1 dx' \exp \{ \beta \Phi(x') \} \exp \left\{ \frac{1}{2T_n} [\Phi(x') - \Phi(x)] \right\} \times K_0 \left\{ \frac{1}{2T_n} |\Phi(x') - \Phi(x)| \right\}, \quad (6)$$

where $K_0(z_1)$ is the zero-order modified Bessel function. Its expansions for the small and large arguments are

$$K_0(z_1) \simeq \ln \frac{2}{z_1 \gamma_E} + O(z_1^2), \quad z_1 \ll 1, \quad (7)$$

$$K_0(z_1) \simeq \sqrt{\frac{\pi}{2z_1}} e^{-z_1} \left\{ 1 + O\left(\frac{1}{z_1}\right) \right\}, \quad z_1 \gg 1. \quad (8)$$

Here $\gamma_E = \exp(c_E) = 1.78107$, $c_E = \lim_{n \rightarrow \infty} \sum_{i=1}^n 1/i - \ln n$ is the Euler constant. For the **ion-source of the symmetric “water-bag”** type, the auxiliary function is

$$F_n\left(\frac{v}{v_{T_n}}\right) = \sqrt{\frac{\pi}{6}} \left\{ H\left(v + \sqrt{\frac{3}{2}T_n}\right) - H\left(v - \sqrt{\frac{3}{2}T_n}\right) \right\}. \quad (9)$$

For the ion density from Eqs. (1) and (9), we find

$$\begin{aligned} n_i(x) = & \sqrt{\frac{2\pi}{3}} B \left\{ \int_0^x dx' \exp[\beta\Phi(x')] \right. \\ & \times \text{arcSh}\left(\frac{\sqrt{3T_n}}{\sqrt{2[\Phi(x') - \Phi(x)]}}\right) \\ & + \int_x^1 dx' \exp[\Phi(x')] \text{arcSh} \\ & \times \left(\sqrt{\frac{3T_n}{2[\Phi(x') - \Phi(x)]} - 1}\right) \\ & \left. \times H\left(\sqrt{\frac{3T_n}{2[\Phi(x') - \Phi(x)]} - 1}\right) \right\}. \quad (10) \end{aligned}$$

For small and large arguments, we assume

$$\text{arcSh}(z_2) \simeq z_2, \quad z_2 \ll 1, \quad (11)$$

$$\text{arcSh}(z_2) \simeq \ln(2z_2), \quad z_2 \gg 1. \quad (12)$$

The definition of the potential shape in the region close to the sheath edge, we start from the pre-sheath (plasma) equation,

$$n_e - n_i = 0, \quad (13)$$

with above-defined ion density distributions and Boltzmann distributed electrons $n_e = \exp[\Phi(x)]$.

Our task is to define the character of the singularity at the sheath edge and find power α in the relation

$$\Phi - \Phi_s = C(x_s - x)^\alpha, \quad (14)$$

where x_s and Φ_s are the sheath edge coordinate and the potential there, assuming that they as well as α and C are the parameters that depend on the ion source temperature.

A. Limit of cold ion-sources

For the cold ion-source with a negligible neutral temperature, $T_n \rightarrow 0$, Eqs. (6) and (10) by means of Eqs. (8) and (11) must give the same result and really in both the

Maxwellian and the “water-bag” cases for the ion density at $T_n \rightarrow 0$, we find

$$n_i(x) = \sqrt{\pi} B_0 \int_0^x dx' \frac{\exp[\beta\Phi(x')]}{\sqrt{\Phi(x') - \Phi(x)}}, \quad (15)$$

which together with Eq. (13) yields the plasma equation in the form

$$\sqrt{\pi} B_0 \int_0^\Phi \frac{dx'}{d\Phi'} \frac{\exp[\beta\Phi(x')]}{\sqrt{\Phi(x') - \Phi(x)}} d\Phi' = \exp[\Phi(x)], \quad (16)$$

with solution [see, e.g., in Riemann 2006 (Ref. 13)]

$$\frac{dx}{d\Phi} = \frac{2}{\pi} \exp(-\beta\Phi) \left[F_D(\sqrt{-\Phi}) - \frac{1}{2\sqrt{-\Phi}} \right], \quad (17)$$

where

$$F_D(z) = e^{-z^2} \int_0^z e^{t^2} dt \quad (18)$$

is the Dawson function.³⁰ Singularity of the electric field defined by Eq. (17) appears for $2F_D(\sqrt{-\Phi_s}) - 1/\sqrt{-\Phi_s} = 0$, yielding

$$\Phi_s = -0.85403... \quad (19)$$

Explicit solution of Eq. (17) for $\beta = 0$ (uniform ionization) and $\beta = 1$ (ionization proportional to electron density) is

$$x = \begin{cases} \frac{2}{\pi} F_D(\sqrt{-\Phi}), & \beta = 0 \\ \frac{e^{-\Phi}}{\pi} \left[(1 + 2\Phi) F_D(\sqrt{-\Phi}) + \sqrt{-\Phi} \right], & \beta = 1 \end{cases} \quad (20)$$

yielding famous numerical values

$$x_s = \begin{cases} \frac{1}{\pi\sqrt{-\Phi_s}} = 0.34444... & \beta = 0 \\ \frac{e^{-\Phi_s}}{2\pi\sqrt{-\Phi_s}} = 0.40456... & \beta = 1 \end{cases} \quad (21)$$

obtained for the first time by Harrison and Thompson²⁵ (being the system lengths, i.e., ionization lengths²⁰) normalized to unity. The numerical values of H&T are for the multiplicative factor $\sqrt{2}$ less than in all Riemann's works.

It is now straightforward to expand into Taylor series $x(\Phi)$ in the vicinity of $x_s(\Phi_s)$, resulting in

$$x - x_s = -\frac{e^{-\beta\Phi_s}}{4\pi\Phi_s^{3/2}} (\Phi - \Phi_s)^2, \quad (22)$$

i.e.,

$$\Phi - \Phi_s = (x - x_s)^{1/2}, \quad (23)$$

with $C_{\beta=0} \approx 3.15$ and $C_{\beta=1} \approx 2.055$ and the exact value, i.e.,

$$\alpha = 1/2, \quad (24)$$

characterizing the potential shape near the singularity point in the case of the cold ion-source. We note here that if Riemann's normalization is used, constants C take other values, i.e., $C_{\beta=0} \approx 2.659$ and $C_{\beta=1} \approx 1.728$, respectively. However, if the system is considered to be equal unity ($L \simeq L_i$) as in all numerical calculations, the ionization length is normalized to L , so that relevant constants in the present investigations are

$$C_{\beta=0} \approx 1.8486, \quad C_{\beta=1} \approx 1.3069 \quad (25)$$

The last values are important for a subsequent comparison with our numerically obtained results.

B. Limit of warm ion-sources

In the case of a high ion source temperature, i.e.,

$$T_n > |\Phi_s| \geq |\Phi - \Phi'| \quad (26)$$

via employing expansions (7) and (12), we obtain from expressions (6) and (10) for the Maxwellian source case

$$n_i(x) = B \int_0^{\Phi_s} d\Phi' \frac{dx(\Phi')}{d\Phi'} \exp[\beta\Phi(x')] \times \exp\left\{ \frac{1}{2T_n} [\Phi(x') - \Phi(x)] \right\} \ln \frac{4T_n}{|\Phi(x) - \Phi(x')|}, \quad (27)$$

and for the “water-bag” ion source case

$$n_i(x) = \sqrt{\frac{2\pi}{3}} B \int_0^{\Phi_s} d\Phi' \frac{dx(\Phi')}{d\Phi'} \exp[\beta\Phi(x')] \times \ln \sqrt{\frac{6T_n}{|\Phi(x) - \Phi(x')|}}, \quad (28)$$

respectively. The plasma (pre-sheath) equation $n_i = n_e$ can be presented in a general form

$$\int_0^{\Phi_s} d\Phi' \frac{dx'}{d\Phi'} \exp[(b-1)\Phi'] \exp[a(\Phi' - \Phi)] \ln \frac{bT_n}{|\Phi' - \Phi|} = c\sqrt{T_n}, \quad (29)$$

where the constants a , b , c are defined for the **Maxwellian source** as

$$a = \beta + \frac{1}{2T_n}, \quad b = \frac{4}{\gamma_E}, \quad c = \frac{1}{B_0}, \quad (30)$$

and for the “water-bag” source in the form

$$a = 1, \quad b = 6, \quad c = \sqrt{\frac{6}{\pi}} \frac{1}{B_0}, \quad (31)$$

with B_0 as defined from Eq. (2), and Φ_s is the potential at the singularity point of the electric field. Further, we note the properties as follows:

- (1) Really the derivative of Eq. (29) with respect to Φ at the sheath edge equals zero,

$$\left. \frac{dx}{d\Phi} \right|_{\Phi=\Phi_s} = 0, \quad (32)$$

meaning that the electric field has singularity at $\Phi = \Phi_s$.

- (2) We assume that $x = 0$ is an extremum (maximum) point of the potential. Then

$$\left. \frac{dx}{d\Phi} \right|_{\Phi=0} = \infty. \quad (33)$$

- (3) Derivative of Eq. (29) with respect to Φ is also zero. In fact, this derivative acts only on the part of the integrand, which depends on the difference $\Phi' - \Phi$. Therefore, this derivative under the integral can be replaced with the derivative with Φ' ,

$$\int_0^{\Phi_s} d\Phi' \frac{dx'}{d\Phi'} \exp[(b-1)\Phi'] \frac{d}{d\Phi'} \exp[a(\Phi' - \Phi)] \times \ln \frac{bT_n}{|\Phi' - \Phi|} = 0. \quad (34)$$

Using Eq. (32) after the partial integration from Eq. (34), we find

$$\int_0^{\Phi_s} d\Phi' \frac{d^2x}{d\Phi'^2} \exp[(b-1)\Phi'] \exp[a(\Phi' - \Phi)] \ln \frac{bT_n}{|\Phi' - \Phi|} = -(b-1)c\sqrt{T_n} - \left. \frac{dx}{d\Phi'} \right|_{\Phi'=0} \exp[a\Phi] \ln \frac{bT_n}{|\Phi|} \rightarrow -\infty. \quad (35)$$

In Appendix, we show that the point $\ln(\Phi' - \Phi)$ as $\Phi' \rightarrow \Phi$ does not lead to the divergence of the integral on the left side of Eq. (35). The divergence of the integral can occur at the expense of the singularity of the function $d^2x/d\Phi^2$ at some point. As the basic assumption of the present model is that the potential is a monotonic function in the interval $0 \leq x < x_s$, we may expect that the point $x = x_s$, where $\Phi = \Phi_s$, is the singular point of the function $d^2x/d\Phi^2$, which will be shown below,

$$\left. \frac{d^2x}{d\Phi^2} \right|_{\Phi=\Phi_s} = -\infty. \quad (36)$$

Presenting Eq. (14) in the form

$$x = x_s - C^{-1/\alpha} (\Phi - \Phi_s)^{1/\alpha}, \quad (37)$$

the relation (32) appears to be valid only for $1/\alpha > 1$, and the relation (36) gives $1/\alpha < 2$. So summarizing the conclusions of items (1) and (3), it follows that fulfillment of relations (32) and (36) require power α to be in the interval

$$1 > \alpha > 1/2. \quad (38)$$

- (4) The derivative of Eq. (29) with respect to Φ can also be presented in a different form

$$\int_0^{\Phi_s} d\Phi' \frac{dx'}{d\Phi'} \frac{\exp[-a(\Phi - \Phi')] \exp[(b-1)\Phi']}{\Phi' - \Phi} = ac\sqrt{T_n}, \quad (39)$$

where the r.h.s. is obtained after the derivation of the exponential function in the integrand of Eq. (29).

To simplify the analytic investigations, we further consider the ion-sources with high temperatures, $T_n \gg 1$.

According to the results by Ref. 20 (Fig. 8) and Ref. 3, at increasing temperatures, the absolute value of the boundary potential Φ_s decreases and $|\Phi_s| \ll 1$ for $T_n \gg 1$. From Eq. (30), there is also $a \simeq 1$. Supposing in Eq. (39) $\Phi = \Phi_s$, we obtain

$$\int_0^{\Phi_s} d\Phi' \frac{dx'}{d\Phi' \Phi' - \Phi_s} = c\sqrt{T_n}. \quad (40)$$

Substituting Eq. (37) into Eq. (40) and introducing the new variable $s = |\Phi'|/T_n$, we obtain

$$T_n^{\frac{3}{2} - \frac{1}{\alpha}} \simeq \frac{1}{cC^{1/\alpha}\alpha} \int_0^{|\Phi_s|/T_n} ds \left\{ \frac{|\Phi_s|}{T_n} - s \right\}^{\frac{1}{\alpha} - 2}. \quad (41)$$

We assume that for $T_n \gg 1$, the dependence of C on the temperature is smooth (from Fig. 10, it follows that such an assumption can be justified). According to the results of Ref. 31 (Fig. 3) and Ref. 20 (Fig. 8), the absolute value of the boundary potential Φ_s might be assumed to decrease approximately linearly with the increase of the temperature in the high temperature region. Then the ratio $|\Phi_s|/T_n$ and therefore the whole r.h.s. of Eq. (41) do not depend of T_n . We can conclude that the relation (41) as equality can be fulfilled only for $\alpha = 2/3$.

In general, we want to mention that the assumptions and conclusions made above are confirmed by numerical calculations presented in Sec. III.

C. Region of medium temperature ion-sources

An expansion of modified Bessel function $K_0(z)$ shows that already for $z \leq 0.5$, the higher order terms might be considered as rather small since for $z = 0.5$ the logarithmic term is $\ln z \simeq 0.65$ and the next term of expansion $z^2/4 \simeq 0.063$ (e.g., Ref. 32). Therefore, one may consider that expression $|\Phi - \Phi'|/2T_n < 0.5$ or even a more conservative condition $T_n > |\Phi_s|$ is a good estimation of the ‘‘warmness’’ of the ion source. It will turn out from our numerical results that this estimation is a crude over-restriction.

III. NUMERICAL METHOD AND NUMERICALLY OBTAINED SHEATH EDGE PROPERTIES

We solve the basic plasma equation of the ‘‘generalized’’ Bissell and Johnson model

$$\frac{1}{B} = \int_0^1 dx' \exp \left[\left(\beta + \frac{1}{2T_n} \right) \Phi(x') - \left(1 + \frac{1}{2T_n} \right) \Phi(x) \right] \times K_0 \left(\frac{1}{2T_n} |\Phi(x') - \Phi(x)| \right), \quad (42)$$

where generalization consists in parameter β , which characterizes the ionization mechanism distribution and takes, e.g., value $\beta = 0$ for uniformly distributed ion source and $\beta = 1$ for the ion source proportional to the electron density [see, e.g., Jelić *et al.*, 2009 (Ref. 20)]. Since the potential profile is dependent on the ionization source, we here investigate the difference of the results for cases $\beta = 0$ and $\beta = 1$. The determination of α simultaneously with constant C_{T_n} was

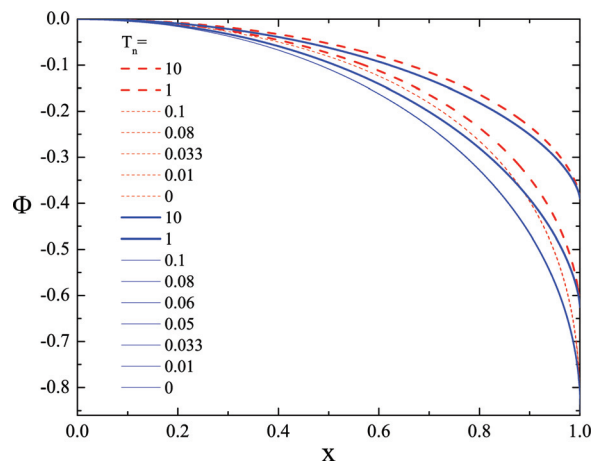


FIG. 3. (Color online) Potential profiles for $\beta = 0$ (dashed) and $\beta = 1$ (solid) in the whole calculation range.

performed via the given model fitted with a different number of end-points. The main question concerning a numerical determination of sheath edge singularity is focused on the qualitative and quantitative determination of potential profiles $\Phi(x)$. We have to find with high reliability the power alpha and constant C in the formula (14) describing the limiting potential variation in front of the sheath edge (x_s, Φ_s) for $T_n > 0$. Before that, it is necessary to decide what algorithm is appropriate for reliable carrying out this task. In order to do so, one has to be systematically familiarized with the properties of the sheath edge for finite T_n .

In Fig. 3, we present the potential profiles obtained for $\beta = 1$ (solid lines) and $\beta = 0$ (dashed lines) in a wide range of ion source temperatures. For any of particular T_n , potential profiles start at $\Phi = 0$ and ends at Φ_s independently of value of β . However, with exception of these end points, the curves differ in all other points, reflecting the well-known property of the T&L solution that the plasma solution is invariant with respect to potential but is *not* invariant with respect to the spatial coordinate. Second, it is obvious that for very small T_n , the said pairs of curves are so close to each other that at Fig. 3, these pairs are indistinguishable and almost coincide with case $T_n = 0$. The pairs obtained for $T_n = 0.1$ and $T_n = 1$ are clearly distinguishable from said ‘‘cluster’’ of curves near $T_n = 0$. For this reason, we inspect curves for $T_n \leq 0.1$ in a strongly magnified scale as illustrated in Fig. 4, where the case $\beta = 0$ is made invisible for clearance. An important fact to be noted is that the numerically obtained curve for $T_n = 0.01$ is an excellent approximation of the exact analytic curve for $T_n = 0$, so that for practical purposes, they might be substituted each by another.

Our code employs the piecewise Lagrangian interpolation of order 2 or 3 in the areas of mild $\Phi(x)$ gradients, so we can perform iterations with high accuracy within wide ion-source temperature ranges, especially in the limit $T_n \rightarrow 0$, which is sensitive to instabilities due to the prolonged integration intervals caused by $1/T_n$ singularity [see Eq. (42)] in the kernel. Estimation of α was performed by a non-linear model fitting with a different number of discretization end-points. As expected, the width of approximation near the sheath edge should be sufficiently small to

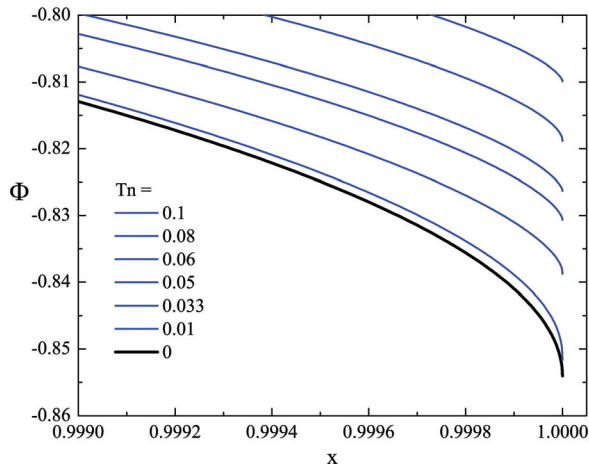


FIG. 4. (Color online) Potential profiles from the previous figure for $\beta = 1$ magnified so that curves obtained for small T_n are clearly distinguishable from each other. Curves obtained for $\beta = 0$ were made invisible at this zoomed view.

characterize singularity and sufficiently large to minimize uncertainty. To analyze these properties, both cold and warm ion-source models are matched under the same “numerical” conditions.

For zero ion-source temperature $T_n = 0$, exact solution in Eq. (20) is used with a valid Φ range from 0 to $\Phi_s = -0.8540326565981972$, which gives the system length of Eq. (21). For a comparison with normalized system length $L = 1$, inverse function $\Phi(z)$ can be numerically solved by finding the root of $z - x(\Phi)/L_0 = 0$. Although Eq. (20) can be evaluated to arbitrary precision, we took approach that is compatible with our code, namely, using higher precision for Eq. (20) and saving a potential profile in the file with compatible precision. To simulate high grading near the sheath edge used in the warm case, the potential curve is positioned at the following discrete positions

$$x_i = \left(1 - \left(1 - \frac{i}{np-1} \right)^{\lambda_2} \right)^{\lambda_1}, \quad i = 0, 1, \dots, np-1, \quad (43)$$

where number of points np and grading at endpoints λ_1 and λ_2 should be similar to those used in warm case $T_n > 0$. Figure 5 shows behavior of our approximation algorithm applied to the “cold” case, for which the “exact” potential profile can be evaluated at arbitrary precision. When using long double machine precision, approximation errors are inevitable. At least a 30 grid point must be used for correct α estimation with a given number of grid points and density. Fig. 5(a) and inset detail in terms of approximation width $w = x_s - x$. Fig. 5(b) shows the same details in terms of number of approximation points n for selected grading. The grid scale in Fig. 5(b) shows that at least 30 grid points must be used to estimate $\alpha = 1/2$. This corresponds to the approximation width of $w = 0.00003$ as shown in the inset graph of Fig. 5(a). The inset graphs also show that, when ruling out tiny range where uncertainty is high, evaluation close to the theoretical value is possible for a large number of grid

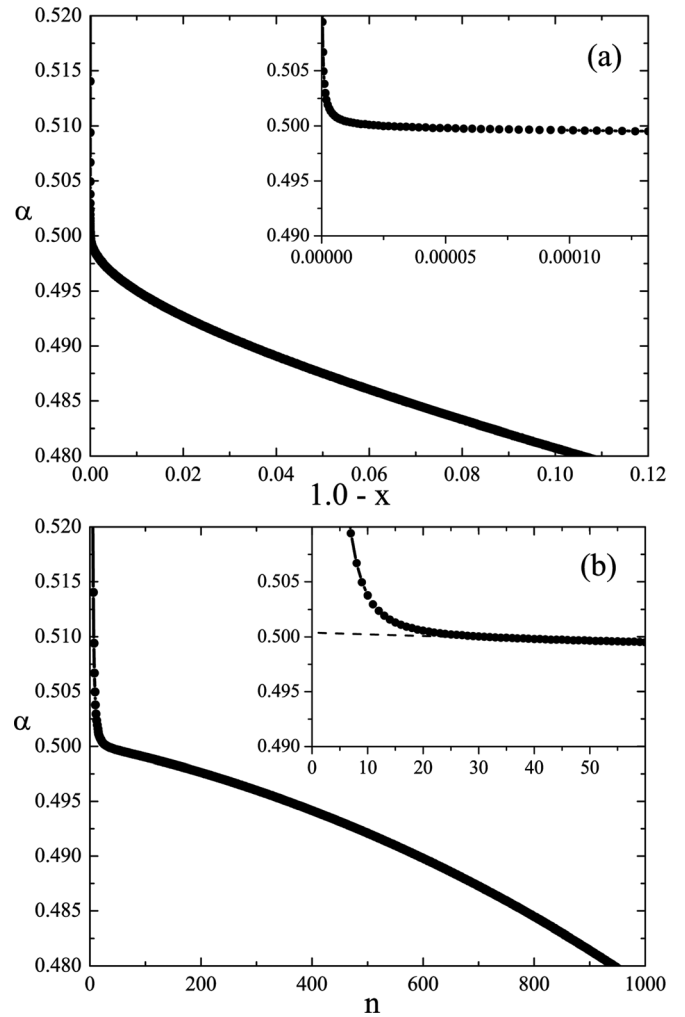


FIG. 5. Approximation of power α for $T_n = 0$ with grid $np = 2401$ points and density $\lambda_1 = 1$, $\lambda_2 = 2.4$. The width of approximation shown in (a) with the same number of points used in approximation n as in grid scale (b). The inset graphs show detailed behavior for evaluation of the α estimation criterion. The dashed line in (b) suggests the extrapolation criterion.

points. This is especially true for the grid scale (b) where also extrapolation criterion can be applied.

While VDF for the cold ion-source is the Dirac δ -function, for the finite ion-source temperatures $T_n > 0$, a variety of VDFs are possible. For the α -approximation, we applied the Maxwellian ion-source, as results were readily available with various grid setups, so we could also test the grid invariance. It turned out that most of the potential profiles near the sheath edge were not accurate enough for α to be reasonably estimated. While all previous parameters (Φ_s, B) converged within 10^5 iterations, the sheath edge detail, from which α is approximated, needs an order of magnitude additional iterations. Fig. 6 shows such α convergence for $T_n = 1$, which took more than three months of computation time on 16 processors compute node and was stopped when convergence to $2/3$ was observed and sufficiently precise results for α were obtained. The calculation of the potential profiles for the whole temperature range and different grids took more than 700 000 processor hours. Fig. 7 shows a similar decreasing function as for the “cold” case in Fig. 5. In contrast with the cold case, we observed here a higher gradient and systematic

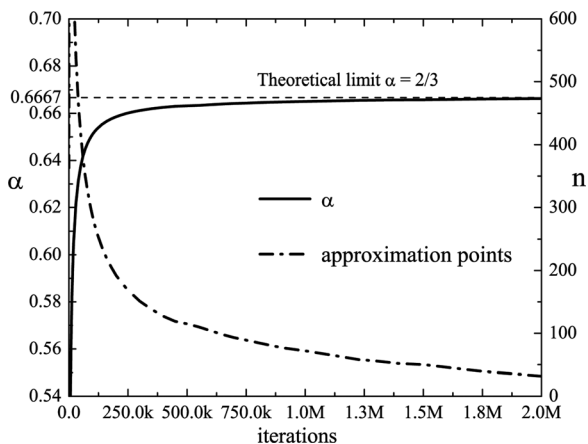


FIG. 6. Convergence of α and a corresponding optimal number of approximation points n .

deflection that underestimates α in the “uncertainty” range. The dashed-dotted line in Fig. 6 shows that the number of approximation points decreases and approaches that of the cold case. The minimal approximation width is thus dependent on the “quality” of the potential profile. We took advantage of the convex function near the sheath edge and resolved with the simple criterion $\alpha = \alpha_{\max}$, which selects the deflection point. When ruling out the “minimal” width, any other estimation criterion can be used to determine the sheath edge singularity in the limit. As seen from the inset graphs, the approximation width is still quite large.

Fig. 8 shows the increase of the grid density at a viewing width $w = 0.0001$ with more than 50 discretization points in the selected range. Origin (0,0) in Fig. 8 is the sheath edge (x_s, Φ_s). Two distinct models are presented: the analytic solution for “cold” $T_n = 0$ T&L model and finite ion-source temperature model with $T_n = 10$. We can safely assume (because we know the analytic solution) that alpha is exactly $1/2$ for $T_n = 0$. The analytic potential profile is discretized to correspond to the discretization used in our program code for finite ion-source temperatures.^{6,33} High resolution grading near the sheath edge is required for precise treatment in the area of interest.

We can conclude that in the limit the power law holds and that problems with the appropriate width when approaching $w \rightarrow 0$ are related to numerical uncertainty. Thus, we can find safely the power alpha with proposed approximation and perform even better if taking into account $\alpha(w)$ variation.

IV. NUMERICAL RESULTS

Dependence of α_{\max} on T_n is shown in Fig. 9 in logarithmic scale. We used different grids to prove invariance of α on the grid setup. For $T_n \geq 0.05$, the approximation came within a couple of percent to the theoretical value of $\alpha = 2/3$. Entirely new result is represented by the transition region observed approximately for $T_n \leq 0.05 \div 0.1$, where we observed a sharp drop of α to another theoretical limit $\alpha_0 = 1/2$. It should be noted that a potential profile for $T_n = 0$ is simulated from the analytic T&L solution and not obtained from our code, and the results agree well with our

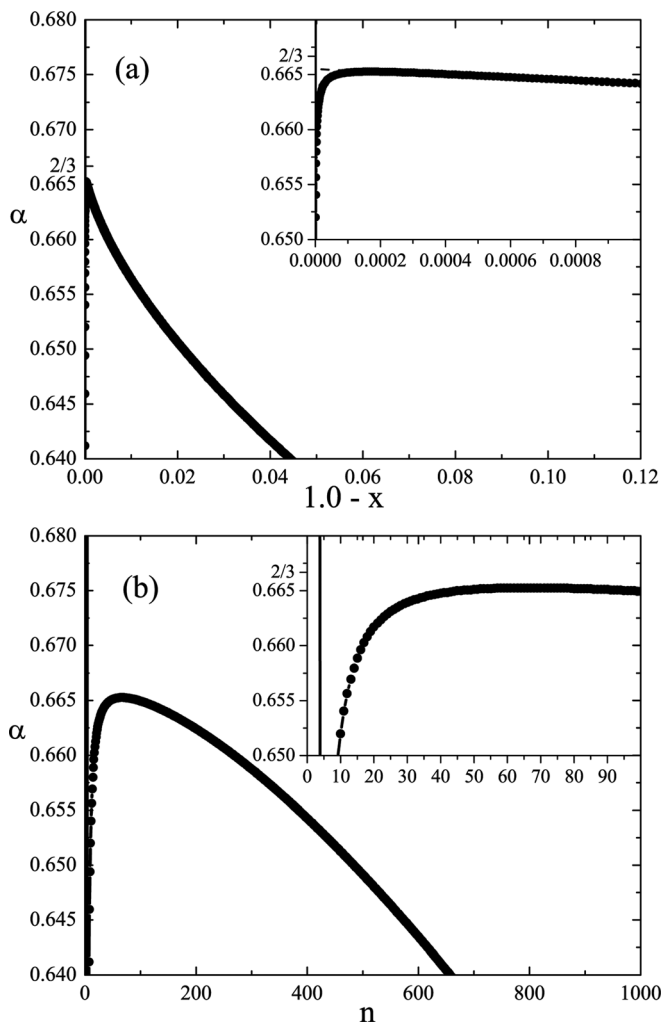


FIG. 7. Approximation of power α for $T_n = 1$ with grid $np = 2401$ points and density $\lambda_1 = 1, \lambda_2 = 2.4$. The width of approximation shown in (a) with the same number of points used in approximation n as in the grid scale (b). The inset graphs show in detail the behavior for the evaluation of the α estimation criterion.

results obtained for very small temperatures. This observation, which is well demonstrated in Fig. 4, additionally supports the reliance of our numerical results. However, the precision of potential profiles in this region of temperatures

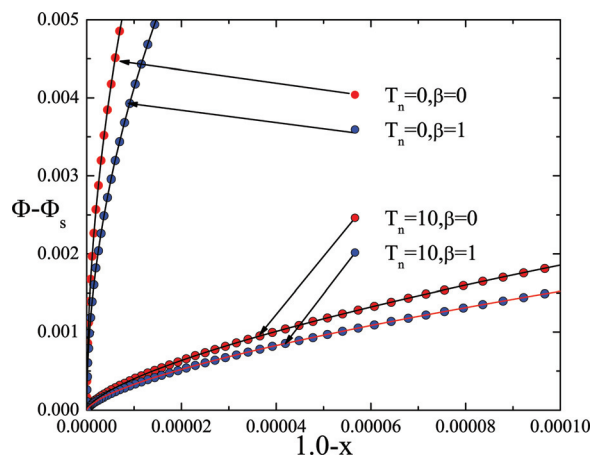


FIG. 8. (Color online) Sheath edge detail for “cold” $T_n = 0$ and “warm” $T_n = 10$ ion-source model.

still could be improved via forcing additional iterations that will even better stabilize α . Precise description of behavior in the region of medium temperatures $0 < T_n \leq 0.1$ also requires a number of additional points, which is a very expensive task that we postpone to be performed in future if deemed necessary for particular purposes, but at the moment, the results presented here meet our needs. For the present purpose, an estimation of linear dependence on α in the region of medium temperatures $0 < T_n \leq 0.0555$ in the form

$$\alpha = \begin{cases} 3T_n + \frac{1}{2}, & T_n < 0.0555\dots \\ \frac{2}{3}, & T_n > 0.0555\dots \end{cases} \quad (44)$$

as illustrated in Fig. 9 seems to be nice and might be useful even for quantitative purposes. Fig. 10 shows the dependence on parameter C_{T_n} on the ion source temperature. The reliability of this result is confirmed by comparing the results obtained from our fitting procedure for very small T_n with theoretical values obtained for $T_n = 0$. These results are the only ones that are reliably known so that the validity of results for C_{T_n} for increasing temperature cannot be checked by an independent method. Thus two very intriguing questions might arise regarding the shape of $C_{T_n}(T_n)$ curves, namely, what is the physical reason why (1) these curves are not monotonic and (2) why the maxima of these curves and the knees of $\alpha(T_n)$ curves are found for approximately the same T_n ($0.05 \div 0.1$)? We must admit that we did not find a satisfactory answer to this question. The only physical difference between strictly cold and approximately cold ion sources is that in the first case, the final ion “temperature” originates from the energy spread due to ion acceleration caused by plasma local potential drop, while in the second case, random motion plays an important role and might dominate over the directional motion. The dependence of final ion temperature T_i on the ion source (neutrals) temperature T_n is illustrated in Fig. 11. Such a dependence in a wider range of temperatures T_n can be found in the work by Kos *et al.*,⁶ where it is clearly seen that with a decreased ion source temperature profiles, $T_i(\Phi)$ monotonically decrease as one approaches from the center towards the plasma boundary. Non-monotonic behavior appears for very low but finite

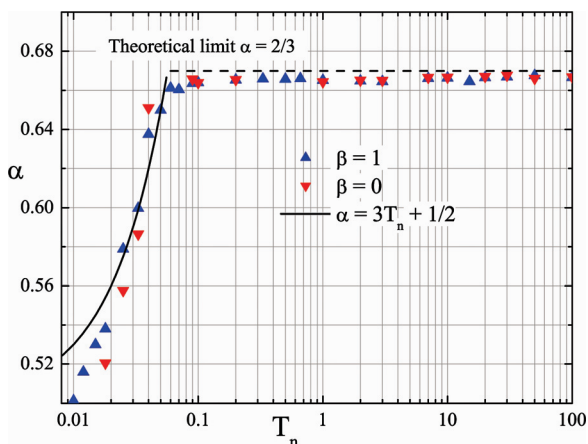


FIG. 9. (Color online) Dependence of power α on the ion-source temperature T_n in logarithmic scale.

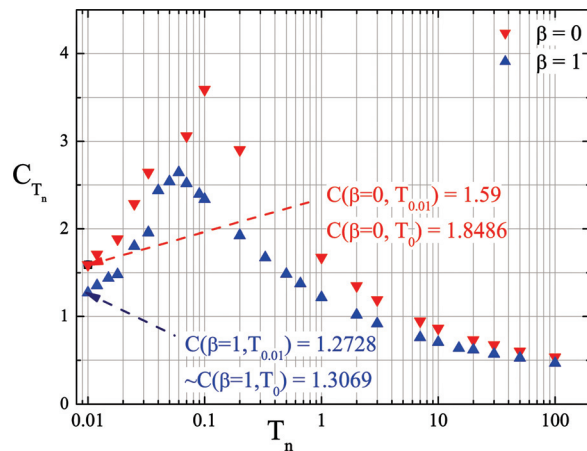


FIG. 10. (Color online) Dependence of the constant C on the ion-source temperature T_n .

ion temperatures. Any physical explanation of the transition region in-between should be related to the qualitative behavior of ion population being not direct but just an *indirect* consequence of the ion-source temperature. Second, the potential profile, especially near the plasma sheath boundary, depends on both ion stochastic and directional motion, since these motions are directly connected to the ion density distribution and so to the potential profile. So the question is what is a characteristic difference between “cold” and “warm” ion motion near the sheath edge. Fig. 11 shows that with very small neutral temperatures, the ion temperature near the sheath edge does not necessary increase with increased neutral temperature. This results from the competition between the directional and random motions. The contribution of the neutral random motion to the total ion temperature is always dominant in the center of the plasma, while near the sheath edge, it is more complex because a slight increase of the random contribution is followed by a decrease of the sheath potential drop. Consequently, with a slight increase of the random ion, the motion ions acquire less energy at the sheath entrance than in the cold neutral case. So, quite surprisingly, the sum of random and directional energy near the sheath

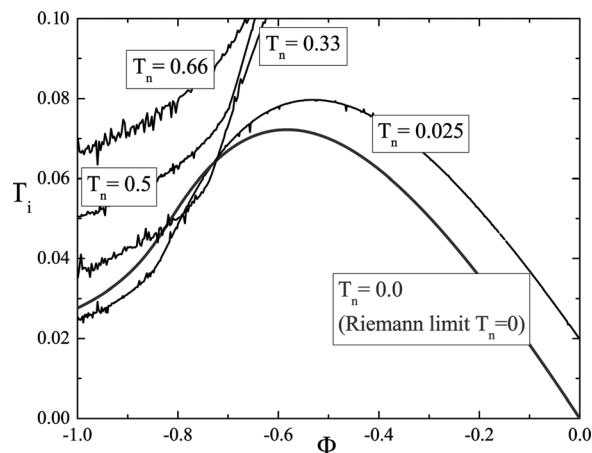


FIG. 11. Dependence of ion temperature T_i on the local potential for small ion-source temperatures T_n .

edge might be lower than in the cold ion-source case. This behavior is clearly illustrated in our Fig. 11: while for increased ion-source temperature, the total ion temperature increases at *any* point (e.g., curves $T_n = 0.66$, $T_n = 0.50$, and $T_n = 0.33$ are one above other, respectively), without any touching or intersecting each other, in cases $T_n = 0.33$, $T_n = 0.025$ there is an “inverse” behavior in the vicinity of the sheath edge and these curves intersect $T_n = 0$ curve and each other.

A possible separatrix of the described two behaviors might be estimated as the “critical” ion source temperature, but we will not perform this task even if this possible separatrix falls in the $T_n = 0.05 \div 0.1$ region, because we are aware that this will not prove anything. Anyway, we draw attention to the “temperature inversion” effect as the only one that we found to be strongly related to the ion-source temperature increase from singular to regular ion-source cases.

V. DISCUSSION AND CONCLUSION

The problem of value in the power law for determining the potential profile near the plasma singularity point is solved for particular Maxwellian and water-bag velocity distributions via both the appropriate analytic approximation method and numerical calculations. The results show that with “cold” ion sources in both particular cases of velocity distribution functions, the dependence $x(\Phi)$ is parabolic (power $1/\alpha = 2$), while in the case of “warm” ion sources, it is fractional (power $1/\alpha = 3/2$). Moreover, this holds independently on the uniformity of the ion source strength. There is a very narrow region between these two limiting cases which we are unable to describe with the analytic method and where the power law can be derived only via the numerical method. Finding a reliable empirical formula in the intermediate region (between high and vanishing ion source temperatures) is a task postponed for the future. For the present purposes, we recommend adopting a linear dependence α_n for $0 < T_n < 0.1T_e$. Our analytic and numerical procedure for the first time estimates the previously unknown width of the “gap” between high and small ion source temperatures where none of fractional power is appropriate for approximating the potential profile. Second, in contrast with the previous assumption that the power law $\alpha = 2/3$ holds for temperatures satisfying, e.g., $T_n > \Phi_s$ (where $\Phi_s(T_n)$ is the value of the potential at the singularity point x_s), it turns out that this power law holds with high reliability in a much wider range of ion source temperatures, i.e., even for $T_n > 0.05 \div 0.1$.

The old results from 1991 (Ref. 1) according to Riemann may be considered as “more than being just an estimation, but less than being proved.”³⁴ That means that a calculation of the power law for at least one particular ion source velocity distribution has so far remained an opened task to be solved. Our investigation is an explicit calculation via using particular ion source velocity distribution functions, i.e., Maxwellian and water-bag. So his general results may be considered now as finally explicitly confirmed and furthermore extended as valid to a much wider range of validity than supposed up till now.

We propose a crude empirical formula $\alpha = 3T_n + 1/2$ describing the dependence α on T_n in the “gap” between the two solutions obtained analytically and numerically for the rational powers of a potential profile. Due to a very narrow range of validity of this non-rational power dependence, it turns out that estimating the validity of the power law for experimental plasmas should be a rather demanding task, since it is difficult to know the ion source temperature with high reliability. The neutral ion source temperature is for sure not equal to the room temperature but it should be higher due to many binary processes, e.g., charge exchange. It seems to be much “safer” to predict the potential profile in really “warm,” i.e., fusion-like plasmas, than in “ordinary” laboratory plasmas, where the ion-source temperature is low but never zero and never equal to the room temperature. As is the case, it turns out that the concept of high, medium, and low ion temperature should be carefully used in future theoretical and engineering investigations before definitely applying any power law to the boundary of a particular plasma, but the present investigation provides a good basis for a relevant decision on proper α . Finally, we conclude that the present investigation is a new basis for any possible future investigations on scaling laws in the intermediate plasma sheath region.

ACKNOWLEDGMENTS

This work was supported by the European Commission under the Contract of Association between EURATOM and the Austrian Academy of Sciences. It was carried out within the framework of the European Fusion Development Agreement. The views and opinions expressed herein do not necessarily reflect those of the European Commission. This work was also supported by the Austrian Science Fund (FWF) under projects P19333-N16 and P22345-N16 and by the “Georgian Science Foundation Grant Project No. 1-4/16 (GNSF/ST09_305_4-140).” Numerical calculations associated with this work were supported by the Austrian Ministry of Science and Research (BMWF) as part of the UniInfrasstrukturprogramm of the Forschungsplattform Scientific Computing at the Leopold-Franzens Universität (LFU) Innsbruck. The authors are indebted to K.-U Riemann for his permanent advice and instructions on theoretical aspects, as well as raising the question on the form of the sheath edge singularity. The authors are also grateful to Professor J. Duhovnik and Professor S. Kuhn for their support in various aspects of our investigations.

APPENDIX: THE DIVERGENCE PROBLEM

In order to simplify the estimation, we assure that $|\Phi_s| \ll 1$ and consider the integral

$$\int_0^{\Phi_s} d\Phi' \frac{d^2x'}{d\Phi'^2} \ln \frac{bT_n}{|\Phi' - \Phi|} = I. \quad (\text{A1})$$

In the interval of integration, we pick out the point $\Phi' = \Phi$,

$$I = I_1 + I_2, \quad (\text{A2})$$

$$I_1 = \left\{ \int_0^{\Phi-\Delta\Phi} d\Phi' + \int_{\Phi+\Delta\Phi}^{\Phi_s} d\Phi' \right\} \frac{d^2x'}{d\Phi'^2} \ln \frac{bT_n}{|\Phi' - \Phi|}, \quad (\text{A3})$$

$$I_2 = \int_{\Phi-\Delta\Phi}^{\Phi+\Delta\Phi} d\Phi' \frac{d^2x'}{d\Phi'^2} \ln \frac{bT_n}{|\Phi' - \Phi|}. \quad (\text{A4})$$

Assuming that $\Delta\Phi$ is small ($\Delta\Phi > 0$), we can [Eq. (A4)] represent in the form

$$I_2 \simeq \frac{d^2x'}{d\Phi'^2} \Big|_{\Phi'-\Phi} \cdot \int_{\Phi-\Delta\Phi}^{\Phi+\Delta\Phi} d\Phi' \ln \frac{bT_n}{|\Phi' - \Phi|}. \quad (\text{A5})$$

In Eq. (A5), we have used the fact that the function $x = x(\Phi)$ is monotonic in interval $\Phi_s < \Phi \leq 0$. From Eq. (A5), we find

$$I_2 \simeq \frac{d^2x'}{d\Phi'^2} \Big|_{\Phi'-\Phi} 2\{\Delta\Phi \ln bT_n - \Delta\Phi(\ln \Delta\Phi - 1)\} < \infty. \quad (\text{A6})$$

Hence, really the point $\Phi' = \Phi$ does not lead to the divergence of the integral in Eq. (35).

¹K.-U. Riemann, *J. Phys. D: Appl. Phys.* **24**, 493 (1991).

²R. C. Bissell and P. C. Johnson, *Phys. Fluids* **30**, 779 (1987).

³J. T. Scheuer and G. A. Emmert, *Phys. Fluids* **31**, 3645 (1988).

⁴K.-U. Riemann, in *Proceedings of the 62nd Annual Gaseous Electronic Conference, APS Meeting Abstracts* (American Physical Society, Saratoga Springs, New York, 2009), Vol. **54**, p. 1001.

⁵K.-U. Riemann, in his e-mail to L. Kos and N. Jelić, 08/24/2009, Riemann inquires: "... Let me finally address one point that would be of great importance for me. Are your results near the sheath edge sufficiently accurate to identify the form of the sheath edge singularity? [That means: can you find safely the power α in the formula $(\Phi_s - \Phi) = c(x_s - x)^\alpha$ describing the limiting potential variation in front of the sheath edge $\Phi_s(x_s)$]." (2009).

⁶L. Kos, N. Jelić, S. Kuhn, and J. Duhovnik, *Phys. Plasmas* **16**, 093503 (2009).

⁷K.-U. Riemann, "The plasma-sheath transition," Seminar held on January 29 at the Institute of Theoretic Physics, University of Innsbruck, Innsbruck, Austria, 2009.

⁸L. Tonks and I. Langmuir, *Phys. Rev.* **34**, 876 (1929).

⁹I. Langmuir, *Phys. Rev.* **33**, 954 (1929).

¹⁰A. Caruso and A. Cavaliere, *Nuovo Cimento (1955-1965)* **26**, 1389 (1962).

¹¹K.-U. Riemann, J. Seebacher, D. D. Tskhakaya, Sr., and S. Kuhn, *Plasma Phys. Controlled Fusion* **47**, 1949 (2005).

¹²K.-U. Riemann, *Phys. Plasmas* **4**, 4158 (1997).

¹³K.-U. Riemann, *Phys. Plasmas* **13**, 063508 (2006).

¹⁴T. E. Sheridan, *Phys. Plasmas* **8**, 4240 (2001).

¹⁵N. Jelić, K.-U. Riemann, T. Gyergyek, S. Kuhn, M. Stanojević, and J. Duhovnik, *Phys. Plasmas* **14**, 103506 (2007).

¹⁶L. Oksuz and N. Hershkowitz, *Plasma Sources Sci. Technol.* **14**, 201 (2005).

¹⁷R. N. Franklin and J. Ockendon, *J. Plasma Phys.* **4**, 371 (1970).

¹⁸K.-U. Riemann, *Plasma Sources Sci. Technol.* **18**, 014006 (2009).

¹⁹K.-U. Riemann, in his hand-written summary of discussion with N. Jelić on 2008 in Innsbruck, Riemann is looking for a complete plasma and sheath solution obtained either via numerical solving Poisson's equation or via particle in cell (PIC) simulations with instruction to calculate from such obtained results $\omega = \varepsilon^{-4/7}(\Phi - \Phi_s)$ and $\zeta = \varepsilon^{-6/7}(x - x_s)$ "... and plot $\omega(\zeta)$ for various ε . Is there a more or less common region? If this common region exists it confirms my prediction on the intermediate scale for hot ion sources." (2009).

²⁰N. Jelić, L. Kos, D. D. Tskhakaya, Sr., and J. Duhovnik, *Phys. Plasmas* **16**, 123503 (2009).

²¹S. Robertson, *Phys. Plasmas* **16**, 103503 (2009).

²²D. Tskhakaya and S. Kuhn, *Plasma Phys. Controlled Fusion* **47**, A327 (2005).

²³A. V. Chankin, D. P. Coster, R. Dux, C. Fuchs, G. Haas, A. Herrmann, L. D. Horton, A. Kallenbach, M. Kaufmann, A. S. Kukushkin, K. Lackner, H. W. Müller, J. Neuhauser, R. Pugno, and M. Tsalias, *J. Nucl. Mater.* **363-365**, 335 (2007).

²⁴D. Bohm, *The Characteristics of Electrical Discharges in Magnetic Fields*, 1st ed., edited by A. Guthrie and R. K. Wakerling (McGraw-Hill, New York, 1949), Chap. 2.5, pp. 49–86.

²⁵E. R. Harrison and W. B. Thompson, *Proc. Phys. Soc. London* **74**, 145 (1959).

²⁶I. D. Kaganovich, *Phys. Plasmas* **9**, 4788 (2002).

²⁷R. C. Davidson, *Methods in Nonlinear Plasma Theory* (Academic, New York, 1972).

²⁸M. van Dyke, *Perturbation Methods in Fluid Mechanics* (Academic, New York, 1964), p. 84.

²⁹S. Kaplun, *Fluid Mechanics and Singular Perturbation* (Academic, New York, 1967).

³⁰M. Abramovitz and I. A. Stegun, *Handbook of Mathematical Functions with Formulas, Graphs and Mathematical Tables* (Dover, New York, 1974).

³¹L. Kos, "Extension of collisionless discharge models for application to fusion-relevant and general plasmas," Ph.D. thesis (University of Ljubljana, 2009).

³²S. Gradstein and I. M. Ryzhik, *Summen-, Produkt und Integral-Tafeln*, 1st ed. (Verlag Harri Deutsch, Thun, 1981).

³³L. Kos, J. Duhovnik, and N. Jelić, in *Proceedings of the International Conference Nuclear Energy for New Europe 2009* (Nuclear Society of Slovenia, Bled, Slovenia, 2009), pp. 820.1–820.10.

³⁴K.-U. Riemann, Private discussion with N. Jelić on novelty of our results presented in present paper (2010).